Electroretinographic Anomalies in Mice with Mutations in *Myo7a*, the Gene Involved in Human Usher Syndrome Type 1B

Richard T. Libby and Karen P. Steel

Purpose. In humans, mutations in the gene encoding myosin VIIa can cause Usher syndrome type 1b (USH1B), a disease characterized by deafness and retinitis pigmentosa. Myosin VIIa is also the gene responsible for the inner ear abnormalities at the shaker1 (*sh1*) locus in mice. To date, none of the *sh1* alleles examined have shown any signs of retinal degeneration. In the present study, electroretinograms (ERGs) were recorded from *sh1* mice to determine whether they have any physiological abnormalities.

Methods. ERGs were recorded from mice homozygous for one of nine mutant alleles of *Myo7a* ranging in age from postnatal day (P)20 to approximately 1 year. All mice were dark adapted for 30 minutes, and all the mutant mice were paired with an appropriately age- and strain-matched control animal. A presumptive null allele of myosin VIIa, $Myo7a^{4626SB}$, was used to determine whether mice without myosin VIIa had an increased threshold, as assessed by the light level required to elicit a 15-μV b-wave.

Results. At the maximum light intensity used, five of the nine alleles examined had significantly reduced a- and b-wave amplitudes. For example, $Myo7a^{4626SB}$ mutant mice had a 20% reduction in a-wave amplitude at the maximum light intensity, and this reduction was the same for mice ranging in age from P20 through 7 months. The b-wave thresholds of the $Myo7a^{4626SB}$ mutant mice were not significantly different from those of the control mice. Furthermore, whereas most of the alleles' a-wave implicit times were the same in mutant and control mice, mutant mice with two of the alleles had significantly faster a-wave implicit times.

Conclusions. Mutations in myosin VIIa in mice can lead to decreased ERG amplitudes while threshold remains normal. This is the first report of a physiological anomaly in a mouse model with a mutation in the same gene as involved in USH1B. (*Invest Ophthalmol Vis Sci.* 2001;42:770–778)

Myosin VIIa is an unconventional myosin that presumably functions as an actin-based motor. In humans, mutations in the gene encoding myosin VIIa (*MYO7A*) cause nonsyndromic deafness[1–3] and Usher syndrome.[4,5] Usher syndrome (USH) is one of the most common forms of syndromic deafness and is characterized by hearing loss, retinitis pigmentosa, and in some types, vestibular dysfunction. Mutations in *MYO7A* are responsible for two forms of USH, atypical USH and USH type 1b (USH1B). USH1B is by far the most common form of USH caused by *MYO7A* mutations and is characterized by profound congenital deafness and the prepubertal onset of retinal degeneration.[6] Presently, there are 57 mutations in *MYO7A* spread throughout the molecule that ultimately result in retinitis pigmentosa.[4,5,7–13]

Myosin VIIa (*Myo7a*) has also been identified as the gene involved in deafness at the shaker1 (*sh1*) locus in mice.[14] To date, 10 *Myo7a* mutant alleles have been identified, and all of them have inner ear defects[15,16] (Steel and Self, unpublished observation, 2000). In fact, none of the hair cells of *Myo7a* mutant mice develop normally, and all of them result eventually in profound deafness. Therefore, the *sh1* mouse appears to be a good animal model for the inner ear disease in humans resulting from mutations in *MYO7A*. In contrast to the good correlation between the mouse and human inner ear phenotypes, the retinas of *Myo7a* mutant mice (including presumptive null mutations) show no signs of retinal degeneration.[17,18] Therefore, the *sh1* mouse does not appear to be a good model for the visual defects in USH1B.

In vertebrates, myosin VIIa is expressed in the retinal pigment epithelium (RPE) and photoreceptor cells. Both cell types contain the components of the visual cycle, and abnormal function of either can lead to retinal degeneration.[19] Myosin VIIa is present at the apical surface of the RPE[20–22] and in $Myo7a^{sh1}$ mutant mice, the melanosomes in the RPE do not invade the apical process.[23] This abnormality is not thought to result in retinal degeneration, because other mice with melanosome abnormalities do not normally undergo retinal degeneration.[23] The localization of myosin VIIa to the apical border of the microvilli and the fact that a member of the myosin VII family is involved in phagocytosis in the amoeba *Dictyostelium discoideum*[24] suggests a possible involvement of myosin VIIa in phagocytosis of outer segments; however, no evidence of a disruption of phagocytosis has been found.[23]

In human and mouse photoreceptors, myosin VIIa is localized in the connecting cilium of rods and cones.[22] Despite the expression of myosin VIIa in the connecting cilium of photoreceptors, no ultrastructural defects in these cilia were found in *Myo7a* mutant mice (Cable and Steel, manuscript in preparation). Autoradiographic studies of outer segment disc synthesis showed that the rate of new disc synthesis was significantly reduced in *Myo7a* mutant mice; however, it is important to note that the length of *Myo7a* mutant outer segments is not affected by the slow process of disc renewal.[18] Also this same study showed that opsin abnormally accumulates in the connecting cilium of *Myo7a* mutant mice. Together these data suggest that myosin VIIa is not only present in the connecting cilium of mouse photoreceptors, but also is involved with the transport of opsin and possibly other molecules through the cilium and into the outer segment. Therefore, the *sh1* mouse still appears to be a model for USH1B and also a useful model organism for determining the role of myosin VIIa in the mammalian retina.

We examined by means of electroretinography the retinas of *Myo7a* mutant mice. Their electroretinograms (ERGs) may elucidate a functional problem within the retinas, and if they

From the Medical Research Council Institute of Hearing Research, Nottingham, United Kingdom.

Supported by the Medical Research Council, Defeating Deafness and the European Commission (BMH4-CT96-1324).

Submitted for publication August 4, 2000; revised November 20, 2000; accepted November 30, 2000.

Commercial relationships policy: N.

Corresponding author: Karen P. Steel, MRC Institute of Hearing Research, University Park, Nottingham NG7 2RD, UK.
karen@ihr.mrc.ac.uk

TABLE 1. *Myo7a* Mutant Alleles

Allele	Mutation	Domain	Protein Level	Genetic Background	Origin
sb1	Missense Arg502Pro	Head	0.93	At least 85% CBA/Ca; 15% heterogeneous	Spontaneous
*6J**	Missense Arg241Pro	Head	0.21	75% C57B1/6J; 25% BALBC	Spontaneous
26SB	Missense Phe1800Ile	Tail	0.46†	50% CBA/Ca; 50% BS, some BALBc	ENU-induced
816SB	Intronic del aa 646-655	Head	0.06	50% CBA/Ca; 50% BS, some BALBc	ENU-induced
4494SB	Intronic stop	Head	0.01	50% CBA/Ca; 50% BS, some BALBc	ENU-induced
4626SB	Nonsense Gln720Stop	Head	0.01	50% CBA/Ca; 50% BS, some BALBc	ENU-induced
3336SB	Nonsense Cys2182Stop	Tail	0.13	50% CBA/Ca; 50% BS, some BALBc	ENU-induced
7J	Not known		Not known	C57BL/6J	Spontaneous
8J	Not known		Not known	C57BL/6J	Spontaneous
9J	Not known		Not known	50% C3H MRL-FAS^{lpr}; 50% CBA/Ca	Spontaneous

The mutations and protein levels for *Myo7a*^{7J}, *Myo7a*^{8J}, and *Myo7a*^{9J} are unknown; the mutations and protein levels for the remaining alleles have all been described.[17,25] *Myo7a*^{6J} mice (*) were either from the genetic background shown above or from a cross between these mice and *Mus castaneus.* There appeared to be no difference in the responses of *Myo7a*6J homozygotes on the two different backgrounds (data not shown). Protein levels are expressed as a fraction of the protein level in wild type CBA/Ca mice. Protein levels were from testes and kidney, and the same value was obtained from both tissues for all of the alleles except *Myo7a*^{26SB} (†). The protein level for *Myo7a*^{26SB} was 0.46 in the kidney and 0.18 in the testis, *Myo7a*^{3336SB} was not analysed in this study, because the stock carries an independent retinal degeneration gene, possibly derived from the C3H strain that contributes to the BS inbred strain.

have an abnormal ERG, the specific defect may be useable as predictor of future disease in humans. We found that five of the nine *sb1* alleles examined had decreased ERG amplitudes.

MATERIALS AND METHODS

Animals

Animals were kept in a 14:10-hour light–dark cycle. All animal procedures were conducted in accordance with the ARVO Statement for the Use of Animals in Ophthalmic and Vision Research and in accordance with United Kingdom's Home Office regulations. Strains carrying nine different *Myo7a* alleles were used (Table 1). For six of the alleles, the mutation in *Myo7a* has been determined.[14,25] *Myo7a* mutant mice were distinguished from their control littermates (+/+ or +/*sb1*) by their head-shaking and circling behavior. A total of 122 pairs of mutant mice and control littermates were used in these experiments.

The genetic background of each stock is presented in Table 1. The *N*-ethyl-*N*-nitrosourea (ENU)-induced mutations were derived from ENU treatment of BALBc males, and were repeatedly backcrossed to the BS inbred strain. These mice were kindly provided by Oak Ridge National Laboratories[26] (Oak Ridge, TN). They have since been crossed, once to the CBA/Ca inbred strain to introduce the wild-type allele at the albino locus and intercrossed since then, with most experimental animals reported in this study being derived from the fourth or fifth generation of intercrossing. Selection during intercrossing was based only on the albino and shaker1 loci. As a result, there has been some opportunity for different alleles of other potentially modifying loci to become fixed in the different stocks.

Electroretinography

Mice were anesthetized with urethane (intraperitoneal injection of approximately 2.2 mg/g) and were prepared under room light. The animal was placed into a head holder in a light-tight Faraday cage, and the reference electrode was attached to the head holder. The eyelid was removed, and the pupil was dilated with atropine. After aligning the animal with the light source, a cotton wick electrode coupled to a silver-silver chloride half cell, was placed onto the animal's cornea in a position that minimized any attenuation of the light flash. A test flash was presented to the animal to test the electrode placement. After a 30-minute dark adaptation, animals were presented with one of two series of flashes.

The first ERG light stimulation protocol was designed to limit light adaptation. In this case, recordings were made over 7.8 log units at 0.6-log-unit intervals. The stimulation protocol was: four 50-msec flashes (PS22 Photopic stimulator; Grass, Quincy, MA) separated by 15 seconds for the lowest light levels (7.8–5.4 log units of attenuation); four 50-msec flashes separated by 30 seconds for the intermediate light levels (4.8–3.0 log units of attenuation); and two 50-msec flashes separated by 60 seconds for the brightest light levels (2.4–0 log units of attenuation).

The second ERG light stimulation protocol caused adaptation to occur at the higher light intensities. This protocol consisted of ten 50-msec flashes, that were separated by 3 seconds for every light intensity. A set of recordings for each animal was made over 7.8 log units at 0.3-log-unit intervals, starting with the least bright intensity, and recordings at increasing light levels were made immediately after those at the lower light intensities. In all cases the responses were amplified, recorded, and averaged by computer. The unattenuated flash was 466 candelas (cd)/m^2. The a-wave amplitude was measured from the prestimulus baseline to the minimum value of the first negative deflection, and the b-wave value was measured from the trough of the a-wave (when present) to the maximum positive value. The a- and b-wave implicit times (latencies) were measured from the time of flash onset to either the minimum value of the first negative deflection (a-wave) or to the maximum positive value (b-wave). Because the maximum ERG amplitudes varied with age (see results), two-tailed paired *t*-tests were used to determine whether there was a significant difference of a- and b-wave amplitudes between the mutant and control animals. In all cases, ERGs were performed on a mutant and littermate control consecutively (randomly choosing whether a mutant or a control was performed first). Because there was not a significant relationship between an animal's age and either the a- or b-wave implicit time (see the Results section), two-tailed unpaired *t*-tests were used in implicit time analysis.

RESULTS

Variation in ERG Amplitudes with Age in Normal Mice

Because mice in a wide age range were examined in this study, a post hoc analysis of the relationship between ERG amplitude and age was performed on mice that were examined with the first (nonadapting) of the two protocols used in the study. Amplitudes increased with age up to approximately postnatal day (P)30 and thereafter declined, reaching a steady level by approximately P90 (Fig. 1).

A regression analysis of a-wave amplitude obtained from all the control mice at maximum light intensity versus age (n = 76, P20–P233) showed that a-wave amplitude did not become stable until P90 (Fig. 1; no significant correlation of age with

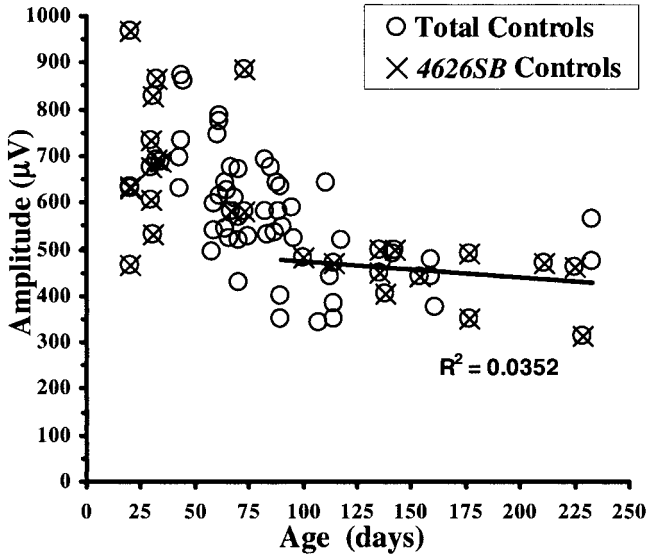

FIGURE 1. The a-wave amplitudes change with age in mice. The a-wave amplitudes at maximum light intensity were plotted versus the age of the mouse for all the control mice from the first (nonadapting) exposure protocol. X, control mice for the *Myo7a*^{4626SB} allele, the largest sample size. In general, the amplitude increased until it reached a peak at approximately P30. After its peak, the amplitude steadily decreased until leveling off at approximately P90. At P90 the amplitude remained steady until at least P233. The *line* on the graph is the best fit line between these time points for all the control mice ($R^2 = 0.0352$, $P = 0.312$). A similarly shaped curve has been reported for rat.[27]

amplitude from P90 through P233; $R^2 = 0.035$, $P = 0.313$). The b-wave amplitude reached its adult level slightly earlier at P85 ($R^2 = 0.021$, $P = 0.410$). The implicit times (latencies) for both the a- and b-waves did not appear to change with age (a-wave $R^2 = 0.005$, $P = 0.528$; b-wave $R^2 = 0.002$, $P = 0.720$), at least over the age range examined in this study. Because several different mouse lines were included in our analysis, a separate analysis that included only mice heterozygous for *Myo7a*^{4626SB} ($n = 28$; P20–P233) was performed. *Myo7a*^{4626SB} heterozygote control animals had results similar to those of the entire control population (Fig. 1). The a-wave and b-wave amplitudes were stable from P100 (no *Myo7a*^{4626SB} control mice were examined between P80 and P99; $R^2 = 0.201$, $P = 0.124$ and $R^2 = 0.004$, $P = 0.835$, respectively). Similar to the total population of control animals, no differences with age were apparent in a- or b-wave implicit times ($R^2 = 0.049$, $P = 0.256$ and $R^2 = 0.015$, $P = 0.501$, respectively). Grossly, the relationship between age and a- and b-wave amplitudes (Fig. 1) is similar to that described by Fulton et al.[27]

Abnormal ERGs in *Myo7a*^{4626SB} Mutant Mice

The mutation in the *Myo7a*^{4626SB} allele results in a stop codon within the head domain, and no protein has been detected in *Myo7a*^{4626SB} mutant mice[17,18,25]; thus, *Myo7a*^{4626SB} is thought to be a null allele. *Myo7a*^{4626SB} homozygotes also have some of the most severe hair cell abnormalities among all the alleles (Steel and Self, unpublished observations, 2000). ERGs were recorded from adult (>P100) *Myo7a*^{4626SB} mutant mice and control littermates ($n = 13$ pairs). The general shape of the ERGs in the mutant mice were the same as in the control animals (Fig. 2A). However, the a-wave amplitude of *Myo7a*^{4626SB} mutant mice was significantly reduced at the higher light intensities compared with control mice (Fig. 2B). A reduced a-wave amplitude for the mutant mice could first be seen at 2.4 log units of attenuation (becoming statistically significant at 1.8 log units; $P < 0.05$) and from this point was approximately only 80% of the control values. As might be predicted, because the b-wave is driven by the a-wave, a reduced b-wave amplitude was seen in the *Myo7a*^{4626SB} mutant mice, although this reduction was not significant until the highest light intensities (Fig. 2C). There was no observable difference in implicit times of the a- or b-waves in mutant mice (Table 2).

No Deterioration with Age of a-Wave Amplitudes of *Myo7a*^{4626SB} Mutant Mice

To determine whether the phenotype (reduced a- and b waves) of the *Myo7a*^{4626SB} mutant mouse changes with age, a series of ERGs were performed on mice ranging from P20 through P229. Because ERG amplitudes varied with age in control animals (Fig. 1), a ratio of the mutant response at the maximum light intensity to that of a control littermate was calculated ($n = 28$ pairs). Throughout the period examined, *Myo7a*^{4626SB} mutant mice had a similar reduction in a-wave amplitude of approximately 20% (Fig. 3). Linear regression of the ratio (mutant response over control response) with age showed no significant correlation ($R^2 = 0.001$, $P = 0.901$). Thus, the ERG phenotype of the mutant mice does not worsen with age.

Normal Thresholds in *Myo7a*^{4626SB} Mutant Mice

Threshold intensities for b-waves of *Myo7a*^{4626SB} were determined using a different light exposure paradigm to that used above. ERGs were recorded from adult *Myo7a*^{4626SB} mutant and control mice (for these experiments control mice were either +/+ or +/*sb1*). In this series of ERGs, 10 flashes at 3-second intervals were averaged at each light intensity, and the light intensity was stepped at 0.3 log units instead of the 0.6 log units used for the 1st paradigm (see the Materials and Methods section for details). This protocol provides average traces with lower noise and finer incremental steps than those of the first protocol, allowing a more precise determination of b-wave threshold. When this protocol was used, adaptation occurred, but not until approximately 2.4 log units of attenuation, and from this point both the a- and b-wave amplitudes of *Myo7a*^{4626SB} mutant mice were significantly less than in the control animals (Fig. 4A). Using this protocol, at maximum responses the mutant amplitude was only 71% and 76% of the control amplitude for the a- and b-wave, respectively ($n = 16$ pairs; aged between P85 and P344) and both the a- and b-waves were significantly attenuated ($P < 0.05$) from 2.4 to 0.0 log units. The mutant and control mice had similar b-wave amplitudes in response to the dimmest light intensities (Fig. 4B). These findings are similar to results obtained using the first ERG protocol. Furthermore, the mutant and control mice required similar levels of light to reach a 15-μV response: 5.79 ± 0.12 log units for mutant and 5.87 ± 0.08 log units for control animals ($P = 0.56$). Therefore, although *Myo7a*^{4626SB} mutant mice had attenuated a- and b-wave responses at the higher intensity flashes, they did not appear to have significantly increased thresholds (reduced sensitivities).

Analysis of Eight *sb1* Alleles

In addition to *Myo7a*^{4626SB}, eight of the remaining nine *sb1* alleles were also analyzed by electroretinography. (*Myo7a*^{3336SB} appears to have a retinal degeneration in its background, unrelated to the *Myo7a* gene, and therefore was not analyzed.) *Myo7a*^{816SB}, *Myo7a*^{7J}, *Myo7a*^{8J}, *Myo7a*^{9J}, *Myo7a*^{4494SB}, *Myo7a*^{6J}, and *Myo7a*^{sb1}, were all analyzed using the first (nonadapting) ERG protocol. Several *sb1* alleles, *Myo7a*^{4494SB}, *Myo7a*^{6J}, and *Myo7a*^{sb1}, did not show any difference in ERGs (with the exception of a significantly faster

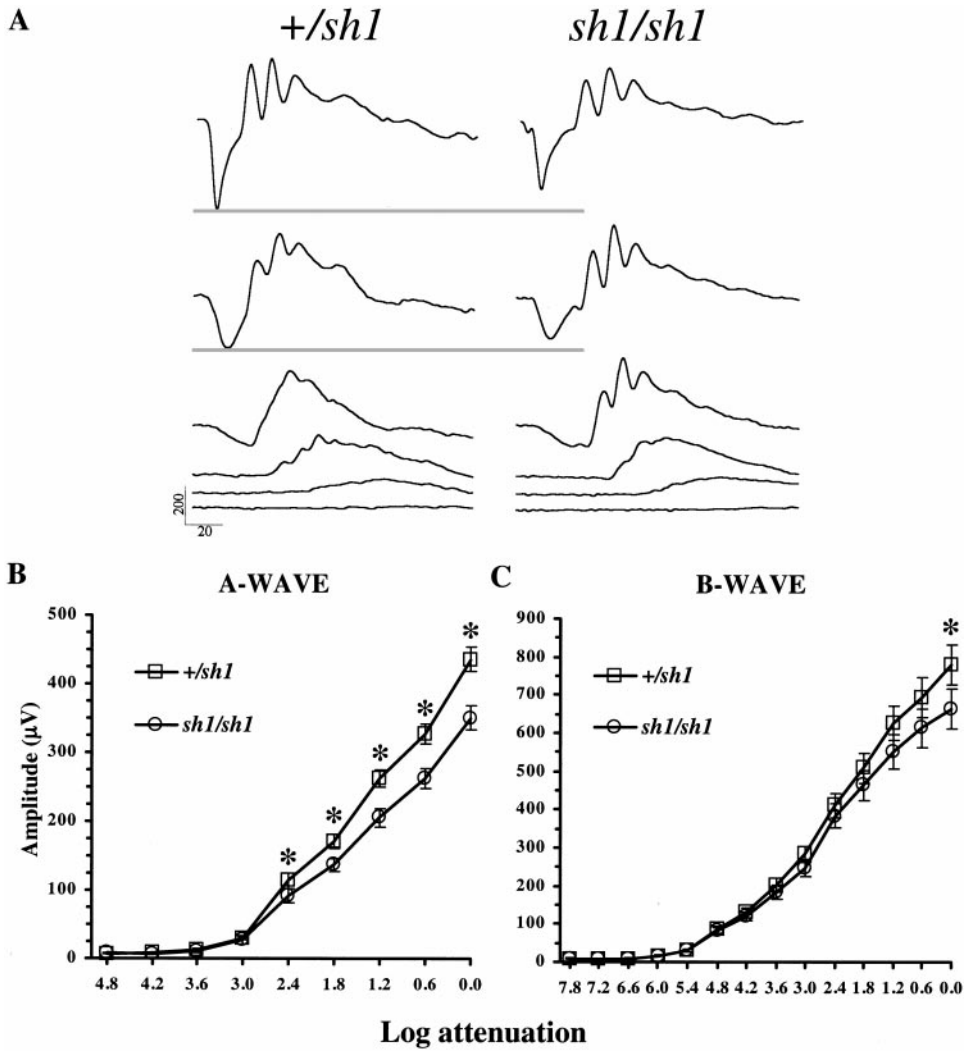

FIGURE 2. *Myo7a*^{4626SB} mutant mice have attenuated a- and b-waves. (**A**) The columns are the averaged responses from an individual mouse using the first (nonadapting) light exposure protocol. The dimmest flash was attenuated by 6.0 log units (*bottom trace*) and was increased at 1.2-log-unit steps until the unattenuated flash (*top trace*). *Left*: Responses from a heterozygous mouse (*+/sh1*) with the response closest to average of all the adult *Myo7a*^{4626SB} control mice; *right*: responses from a *Myo7a*^{4626SB} mutant mouse with the response closest to average for all the *Myo7a*^{4626SB} mutant mice (*sh1/sh1*). *Gray line*: Maximum amplitude of the a-wave at the highest two light intensities in the control mouse, clearly showing that the mutant mice had attenuated a-wave responses. Light onset is at the beginning of the traces. Intensity response curves for a-waves (**B**) and b-waves (**C**) for adult *Myo7a*^{4626SB} mutant and control mice. Mutant a-waves were significantly attenuated from 2.4 log units (*$P < 0.05$), and the b-waves were attenuated from approximately 3.6 log units, but significantly only at the brightest light intensity.

b-wave implicit time in *Myo7a*^{4494SB} mutant mice; Table 2). However, at the brightest light intensity *Myo7a*^{816SB}, *Myo7a*^{7J}, *Myo7a*^{8J}, and *Myo7a*^{9J} mutant mice, similar to *Myo7a*^{4626SB} mutant mice, had significantly reduced a-wave amplitudes (Fig. 5A; Table 2). These animals also had significantly reduced b-wave wave amplitudes (with the exception of *Myo7a*^{816SB}, which was reduced but not significantly), and normal implicit times (with exception of the a-wave implicit time in *Myo7a*^{816SB} and the b-wave implicit time in *Myo7a*^{8J}, which were both significantly faster; Table 2). Also, the alleles that showed a significant difference in a-wave amplitudes at maximum light intensity all showed decreased a-wave amplitudes from 2.4 log units of attenuation (Fig. 5B); the decreased a-wave responses in these mutant mice were significant for all these alleles from 1.8 log units of attenuation up to zero.

The second ERG protocol (the protocol that causes light adaptation) was used on three alleles, *Myo7a*^{4626SB} (discussed earlier), *Myo7a*^{4494SB}, and *Myo7a*^{26SB}. The second light exposure protocol produced similar results for both *Myo7a*^{4626SB} and *Myo7a*^{4494SB} as the first: *Myo7a*^{4626SB} mutant mice had significantly decreased a- and b-wave amplitudes at maximum response (Fig. 4A; Table 2) and *Myo7a*^{4494SB} mutant mice had no difference in a- and b-wave maximum amplitudes compared with control animals (note that their maximum responses occurred by 1.2 log units of attenuation, not at the brightest light intensity; see Fig. 4A for the typical intensity response curve for this light-exposure paradigm). *Myo7a*^{26SB} mutant mice had slightly decreased maximum a- and b-wave amplitudes when the second protocol was used for recording, but these decreases were not significant ($P > 0.05$; Table 2). However, the a- and b-wave implicit times of *Myo7a*^{26SB} mutant mice were significantly faster throughout much of the intensity response curve with the mutant a-waves being significantly faster ($P < 0.05$), from 3.6 to 0.0 log units of attenuation, and the b-wave, from 6.0 to 0.0 log units of attenuation (Table 2 and data not shown).

DISCUSSION

This is the first report of any electrophysiological abnormalities in the retinas of *sh1* mutant mice. The a-wave amplitudes of mice homozygous for five of the nine mutant *Myo7a* alleles examined in this study (*Myo7a*^{4626SB}, *Myo7a*^{816SB}, *Myo7a*^{7J}, *Myo7a*^{8J}, and *Myo7a*^{9J}) were significantly attenuated compared with those of their control littermates. In general, the attenuated a-waves were all reduced by approximately 20% over most of stimulus intensities examined. Because the a-wave of the ERG is the result of photoreceptors responding to light,[28,29] the reduction in a-wave amplitudes suggests that some *Myo7a* mutant mice have abnormal or subnormal photoreceptor function. All the alleles that had attenuated a-waves also had reduced b-waves, which is not surprising. The b-wave of the ERG originates from retinal interneurons[30–32] as a result

TABLE 2. Analysis of ERGs of *Myo7a* Alleles

Allele	Mean age (*n* pairs)	Strain	a-Wave		b-Wave	
			Max Response (μV)	Implicit Time (msec)	Max Response (μV)	Implicit Time (msec)
First protocol						
4626SB	145.6 (16)	*+/sh1*	482.3 ± 32.6 (**0.000**)	12.00 ± 0.24 (0.860)	901.7 ± 94.2 (**0.005**)	50.23 ± 2.05 (0.932)
		sh1/sh1	385.3 ± 27.6	11.74 ± 0.31	748.4 ± 78.5	50.52 ± 2.65
816SB	76.6 (7)	*+/sh1*	633.2 ± 39.5 (**0.014**)	12.61 ± 0.40 (**0.026**)	1202.6 ± 101 (0.140)	54.07 ± 3.82 (0.283)
		sh1/sh1	479.3 ± 22.1	11.25 ± 0.35	997.3 ± 82.9	48.18 ± 3.58
7J	123.9 (10)	*+/sh1*	538.7 ± 35.4 (**0.003**)	11.73 ± 0.26 (0.834)	1072.1 ± 95.1 (**0.013**)	46.15 ± 1.91 (0.581)
		sh1/sh1	370.1 ± 33.7	11.63 ± 0.39	745.7 ± 90.8	48.48 ± 3.65
8J	82.2 (5)	*+/sh1*	652.6 ± 35.0 (**0.012**)	11.95 ± 0.50 (0.094)	1323.5 ± 90.0 (**0.014**)	46.30 ± 1.76 (**0.027**)
		sh1/sh1	536.4 ± 40.2	10.85 ± 0.23	1111.0 ± 106.9	40.50 ± 1.03
9J	47.2 (6)	*+/?*	738.8 ± 42.9 (**0.000**)	11.67 ± 0.179 (0.714)	1500.4 ± 99.0 (**0.034**)	41.58 ± 0.99 (0.886)
		sh1/sh1	533.3 ± 32.9	11.84 ± 0.433	1144.0 ± 83.5	41.94 ± 2.18
4494SB	108.8 (6)	*+/sh1*	530.6 ± 30.6 (0.323)	12.25 ± 0.42 (0.093)	952.7 ± 78.8 (0.195)	50.10 ± 2.09 (**0.005**)
		sh1/sh1	551.3 ± 46.1	11.22 ± 0.37	1046.0 ± 110.1	40.78 ± 1.01
6J	82.1 (9)	*+/sh1*	478.0 ± 38.8 (0.334)	11.69 ± 0.29 (0.495)	896.1 ± 67.0 (0.123)	50.89 ± 2.46 (0.216)
		sh1/sh1	510.8 ± 43.3	11.44 ± 0.20	1013.8 ± 68.7	47.08 ± 1.61
sh1	89.2 (5)	*+/sh1*	487.1 ± 21.2 (0.624)	11.20 ± 0.38 (0.566)	909.6 ± 72.0 (0.818)	47.00 ± 4.55 (0.468)
		sh1/sh1	466.0 ± 28.2	10.90 ± 0.32	940.2 ± 58.0	43.15 ± 1.91
Second protocol						
4626SB	119.9 (19)	*+/?*	255.8 ± 12.8 (**0.003**)	20.00 ± 0.59 (0.699)	548.4 ± 27.5 (**0.004**)	53.44 ± 2.20 (0.347)
		sh1/sh1	179.6 ± 17.2	20.41 ± 0.88	388.6 ± 44.5	49.28 ± 3.73
4494SB	127.7 (13)	*+/?*	251.6 ± 17.4 (0.434)	22.58 ± 1.12 (0.092)	525.5 ± 41.9 (0.392)	50.65 ± 4.84 (0.075)
		sh1/sh1	237.0 ± 19.1	20.35 ± 0.57	489.2 ± 39.1	40.42 ± 2.42
26SB	134.9 (14)	*+/?*	233.7 ± 15.4 (0.163)	23.54 ± 0.79 (**0.001**)	532.5 ± 45.6 (0.398)	59.61 ± 4.23 (**0.018**)
		sh1/sh1	206.6 ± 18.9	19.86 ± 0.52	495.6 ± 38.6	46.46 ± 2.98

Data are means ± SEM with *P* in parentheses. The average maximum obtained responses and their implicit times are shown for each allele and for each light exposure protocol (first or second). For each allele, all mice more than 70 days of age were included in the analysis. The a- and b-wave maximum response *P* is by paired Student's *t*-test, and those for the implicit times are from a unpaired *t*-test. *P* in bold is significant ($P < 0.05$).

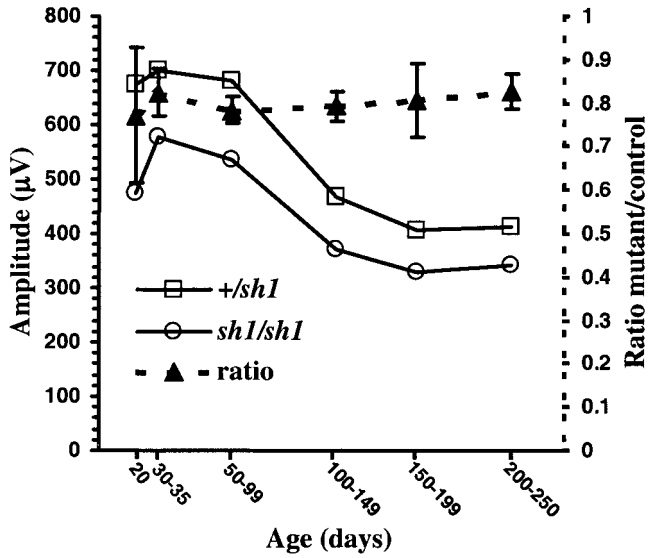

FIGURE 3. The amount of a-wave attenuation of the *Myo7a*^{4626SB} mutant mice did not change during development. ERGs were recorded from 28 pairs of *Myo7a*^{4626SB} mutant mice (*sh1/sh1*) and control littermates (*+/sh1*) ranging in age from P20 to P233. To see whether there is a trend in the amount of attenuation of the mutant mice with age, the pairs of mutant and control mice were split into six age-defined bins. The average a-wave amplitudes at maximum light levels for each bin for the mutant and control mice were plotted along with the ratio between them for each bin. There appeared to be no difference in the ratio throughout the periods analyzed ($R^2 = 0.001$; $P = 0.901$). Error bars for the ratios are ± SEM.

of photoreceptor activity. For at least one allele that had decreased amplitude, *Myo7a*^{4626SB}, there was no change in the level of attenuation of the response between P20 and P233, suggesting that this phenotype does not worsen with age. Furthermore, *Myo7a*^{4626SB} mutant mice did not appear to have raised thresholds. It is interesting that the a-wave implicit times for all the mutant alleles examined were normal, with the exception of *Myo7a*^{816SB}, which was significantly faster, implying that the process of phototransduction occurs at a normal rate in most of the mutant mice.[33] Therefore, the primary finding of this study is that some *Myo7a* mutant retinas have a smaller response to light than do normal mice.

Possible Functions of Myosin VIIa in the Retina

No sign of retinal degeneration has ever been observed in *sh1* mutant mice, even up to 744 days of age.[17,18,23,34] Thus, mutations in the mouse myosin VIIa gene do not appear to cause retinal degeneration, as they do in humans. In both human and mouse retinas, myosin VIIa is expressed in both the cell types that participate in the visual cycle: RPE and photoreceptor cells. In the RPE, myosin VIIa is in the apical processes of RPE cells.[20–22] In *Myo7a*^{sh1} mutant mice the melanosomes in the RPE did not invade the apical process, suggesting that myosin VIIa functions in melanosome transport in the RPE. However, Liu et al.[23] argue that this abnormality is not likely to result in retinal degeneration, because other mice with melanosome abnormalities do not normally undergo retinal degeneration. In photoreceptors, myosin VIIa is concentrated in the connecting cilium of photoreceptors[21,22] and, at least in humans, in the photoreceptor synapse.[21] Myosin VIIa mutant mice have abnormal opsin transport through the connecting cilium revealed by an accumulation of opsin in the cilium and have a rate of new photoreceptor disc synthesis that

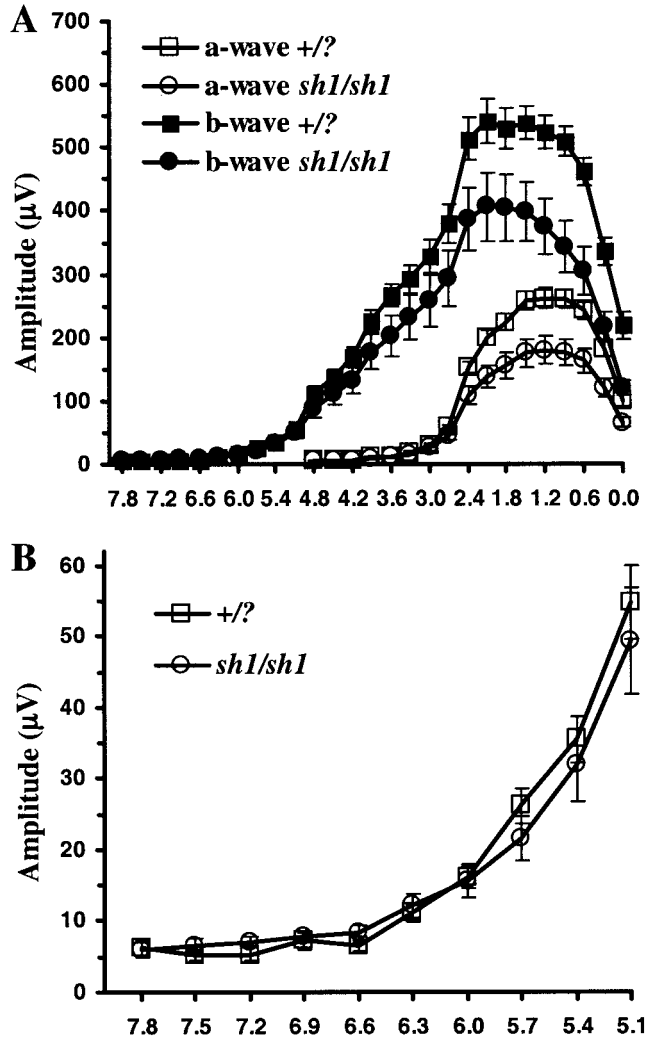

FIGURE 4. *Myo7a*^{4626SB} mutant (*sh1/sh1*) thresholds did not appear to be different from those of the control mice (*+/?*). The second light exposure protocol was used to determine whether b-wave thresholds are raised for the *Myo7a*^{4626SB} mutant mice. In this light exposure protocol 10 flashes with a 3-second interstimulus interval were averaged, and the light intensity was increased in 0.3-log-unit steps. The average intensity response curve for both the a- and b-waves are shown in (**A**). With this protocol the b-wave responses began to be attenuated because of the rapid stimulus repetition at approximately 2.4 log units. The a-wave was significantly different between mutant and control mice from 2.4 to 0 log units and the b-wave from 2.7 to 0 log units. A higher resolution plot of initial stages of mutant and control b-wave response (**B**) shows that in the mutant mice the b-wave mean threshold was the same as in the control animals.

is decreased by approximately 13%. However, these abnormalities do not affect the total amount of opsin expressed in the *sh1* retina or the length of the outer segments.[18] These previous studies show that myosin VIIa functions in both the cell types that are involved in the visual cycle and also in both the cell types in which dysfunction can lead to retinitis pigmentosa.[19]

It is unclear whether either of the previously observed abnormalities could explain the present ERG finding. If the decreased rate of photoreceptor disc synthesis affected the amount of rhodopsin available for phototransduction, we would expect to see an increase in threshold of the ERG,[35,36] but we do not. As for the abnormal accumulation of opsin in the connecting cilium, we can see no mechanism to explain how this could result in a decreased ERG amplitude. Of note, the mouse mutant pearl, similar to some of the *sh1* alleles, has a lack of melanosomes in the apical microvilli of the RPE[37] and has reduced a- and b-wave amplitudes.[38] Pearl mice have abnormalities in the retina that are not seen in *sh1* mutant mice, most notably a reduced total number of melanosomes in the RPE. The gene disrupted in the pearl mouse is the β3A subunit of the AP-3 adapter complex, which functions in cargo-selected transport.[39] Because unconventional myosins are know to be involved in intracellular transport[40] and, in both pearl and *sh1* mutant mice, there are clearly abnormalities in melanosome transport in the RPE, it is tempting to speculate that both myosin VIIa and the AP-3 complex have similar functions in the RPE and that disruptions of these functions lead to reduced ERG amplitudes.

Differences between Human and Mouse

There are several possible reasons that mutations in *MYO7A* in humans can lead to retinal degeneration, whereas in *sh1* mutant mice they do not. (1) The mutations found in human *MYO7A* resulting in USH may be different from those found in mouse *Myo7a*. (2) The genetic background of the particular organism may play a significant role in determining the severity of disease that results from a given mutation in *MYO7A*. (3) Inherent differences between the retinas of the two species could be the reason for different levels of disease. We examine each of these possibilities in turn.

To date, 10 mutant alleles of *Myo7a* have been found (the mutations in 7 of them have been described[14,25]; see Table 1), and more than 57 mutations have been found in human *MYO7A*.[4,5,7–13] Unfortunately, even with this vast array of mutations in both mice and humans, there is no case in which a patient with USH1B has had two copies of a mutation identical with that of one of the *sh1* mouse lines. Until we show identical mutations in the human population and in a mouse line, we cannot be certain that the absence of retinal degeneration in the shaker1 mouse lines is not simply because we do not have the appropriate mutations in *Myo7a*.

In humans, mutations in *MYO7A* are associated with a wide phenotypic spectrum of diseases.[5] These mutations can lead to both dominant[1] and recessive[2,3] nonsyndromic deafness and to two clinically distinct forms of USH, one mild and one severe in effect. Based on there being such a wide range of mutations in *MYO7A* that can result in a fairly broad phenotypic spectrum of diseases, the fact that an identical mutation has been found in both atypical USH and USH1B[5] and that the mutations causing both USH and nonsyndromic deafness are spread throughout the molecule, it has been proposed that genetic background may play an important role in determining the nature of the disease caused by *MYO7A* mutations.[5] Because genetic background may influence the phenotype caused by mutations in *MYO7A* in humans and it is known to affect the inner ear phenotype in *sh1* mutant mice[41] as well as the rate of retinal degeneration in at least one mouse model of a human disease,[42] it is possible that the genetic background is the sole reason for the difference between humans and mice. In this study and in others[17,18] many different alleles of *Myo7a* mutant mice have been examined, but the backgrounds of the alleles are fairly similar (see Table 1).

It is notable that the data presented suggest the possibility that genetic background may affect the manifestation of the ERG phenotype. Both *Myo7a*^{4626SB} and *Myo7a*^{4494SB} are thought to be null mutant mice,[17,18] whereas only *Myo7a*^{4626SB} has attenuated ERG amplitudes. Both presumptive null alleles are on a largely 50% CBA/Ca, 50% BS genetic background. However, the stocks have been maintained by intercrossing within each colony for several generations since

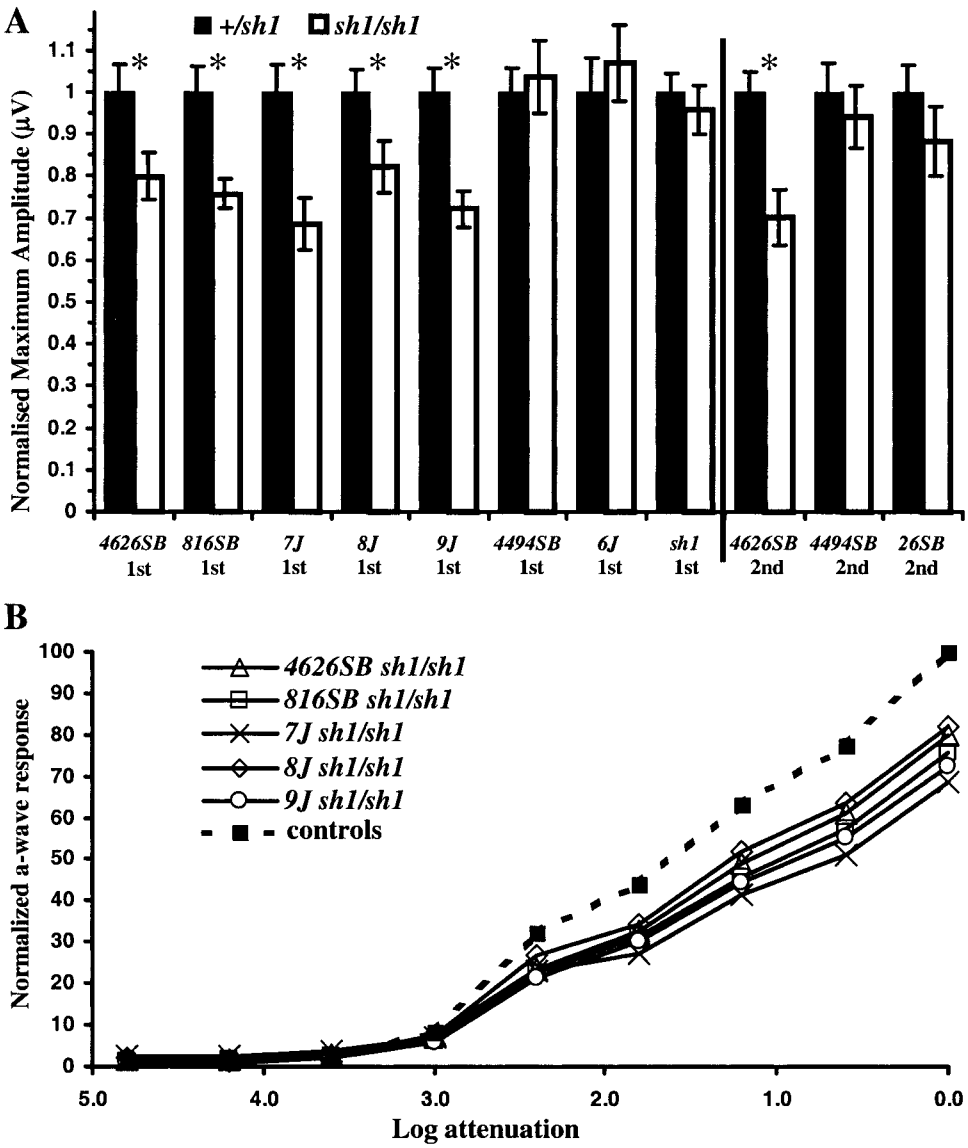

FIGURE 5. Five of the nine *Myo7a* alleles had attenuated a-wave amplitudes. (**A**) Normalized a-wave amplitudes for all the alleles examined are shown. The a-wave amplitudes were obtained from either the first (nonadapting, 1st) or second (adapting, 2nd) protocols, and all amplitudes were the averages of the maximum responses obtained. The a-wave amplitudes of the $Myo7a^{4626SB}$, $Myo7a^{816SB}$, $Myo7a^{7J}$, $Myo7a^{8J}$, and $Myo7a^{9J}$ mutant mice were all significantly less ($^*P < 0.05$) than those of their control mates, whereas those of the $Myo7a^{4494SB}$, $Myo7a^{6J}$, $Myo7a^{7sh1}$, and $Myo7a^{26SB}$ mutant mice were not significantly different from their control littermates. (**B**) The a-wave intensity response curves for all the *Myo7a* alleles that showed a significant difference at the maximum light intensity normalized to the maximum response of the control mice for each allele. The control curve is the averaged normalized response of all the control mice. The mutant mice of these alleles have a similar shape throughout their response; the mutant mice for each allele began to be attenuated in amplitude at approximately 2.4 log units.

the original BS-based stocks were outcrossed to CBA/Ca, and different modifiers from the two backgrounds have therefore most likely become fixed in the stocks. If these two alleles are actually null, then the difference in the ERG amplitudes would have to be the result of the lines' having different modifiers for myosin VIIa. Recently, the first modifiers that effect retinal degeneration have been mapped.[43,44] It will interesting to place the different mutant myosin VIIa alleles onto a background containing these modifiers and determine whether they exacerbate the phenotype observed in *Myo7a* mutant mice.

The difference between the human and mouse phenotypes may simply be that there are intrinsic differences between the two species. One of the more obvious differences between humans and mice is that the first signs of retinal degeneration in patients with USH1B generally occur after they are several years of age, well beyond the life span of a mouse. Kedzierski et al.[45] noted that at least in some retinal degenerations, the rate of degeneration appears to be determined, not by the absolute age of the photoreceptor, but by its relative age compared with the life span of the host species. This observation suggests that the relatively short life span of the mouse may not be the reason there is no degeneration. However, there are several mutant mouse strains in which retinal degeneration is dependent on exposure to light or in which the rate of degeneration can be increased by exposure to light.[46–51] It is possible that the retinas of *Myo7a* mutant mice do not degenerate because they have not been exposed to the same total light levels as the typical human with USH1B, and/or their relatively short life span is not long enough for the necessary accumulation of insult to result in degeneration.

These data are the first evidence of a physiological abnormality in the retinas of *Myo7a* mutant mice. Mice homozygous for several different mutant *Myo7a* alleles have decreased a- and b-wave amplitudes, suggesting that their photoreceptors are not responding properly to light. The implicit time of the mutant mouse's a- and b-wave were generally the same as in the control mouse. In humans with USH1 (there is no molecular characterization of these persons, and the underlying causes therefore may not be mutations in *MYO7A*), multifocal ERGs have shown that they have amplitude losses with normal implicit times.[52] Patients with USH2 and other forms of retinitis pigmentosa have decreased amplitudes and increased implicit times.[52] The electroretinographic findings reported in this study appear to correlate with physiological findings in humans, at least during the early stages of disease. Thus, the *sh1* mouse may provide a useful model for studying at least the

early stages of the retinitis pigmentosa associated with *MYO7A* mutations in humans.

Acknowledgments

The authors thank Bill Brunken, David Williams, Grant Balkema, and Amy Kiernan for helpful comments and advice and Eugene Rinchik, Wayne Frankel, and Ken Johnson for passing on the *sb1* mutants to us.

References

1. Liu XZ, Walsh J, Tamagawa Y, et al. Autosomal dominant nonsyndromic deafness caused by a mutation in the myosin VIIA gene. *Nat Genet*. 1997;17:268–269.
2. Liu XZ, Walsh J, Mburu P, et al. Mutations in the myosin VIIA gene cause nonsyndromic recessive deafness. *Nat Genet*. 1997;16:188–190.
3. Weil D, Kussel P, Blanchard S, et al. The autosomal recessive isolated deafness, DFNB2, and the Usher 1B syndrome are allelic defects of the myosin-VIIA gene. *Nat Genet*. 1997;16:191–193.
4. Weil D, Blanchard S, Kaplan J, et al. Defective myosin VIIA gene responsible for Usher syndrome type 1B. *Nature*. 1995;374:60–61.
5. Liu XZ, Hope C, Walsh J, et al. Mutations in the myosin VIIA gene cause a wide phenotypic spectrum, including atypical Usher syndrome. *Am J Hum Genet*. 1998;63:909–912.
6. Keats BJ, Corey DP. The Usher syndromes. *Am J Med Genet*. 1999;89:158–166.
7. Levy G, Levi–Acobas F, Blanchard S, et al. Myosin VIIA gene: heterogeneity of the mutations responsible for Usher syndrome type IB. *Hum Mol Genet*. 1997;6:111–116.
8. Cuevas JM, Espinos C, Millan JM, et al. Detection of a novel Cys628STOP mutation of the myosin VIIA gene in Usher syndrome type Ib. *Mol Cell Probes*. 1998;12:417–420.
9. Cuevas JM, Espinos C, Millan JM, et al. Identification of three novel mutations in the MYO7A gene. *Hum Mutat*. 1999;14:181.
10. Janecke AR, Meins M, Sadeghi M, et al. Twelve novel myosin VIIA mutations in 34 patients with Usher syndrome type I: confirmation of genetic heterogeneity. *Hum Mutat*. 1999;13:133–140.
11. Weston MD, Kelley PM, Overbeck LD, et al. Myosin VIIA mutation screening in 189 Usher syndrome type 1 patients. *Am J Hum Genet*. 1996;59:1074–1083.
12. Weston MD, Carney CA, Rivedal SA, Kimberling WJ. Spectrum of myosin VIIa mutations causing Usher syndrome type 1b. *Assoc Res Otolaryngol Abstr*. 1998;21:46.
13. Adato A, Weil D, Kalinski H, et al. Mutation profile of all 49 exons of the human myosin VIIA gene, and haplotype analysis, in Usher 1B families from diverse origins. *Am J Hum Genet*. 1997;61:813–821.
14. Gibson F, Walsh J, Mburu P, et al. A type VII myosin encoded by the mouse deafness gene shaker-1. *Nature*. 1995;374:62–64.
15. Lord EM, Gates WH. Shaker, a new mutation of the house mouse (*Mus musculus*). *Am Nat*. 1929;63:435–442.
16. Self T, Mahony M, Fleming J, Walsh J, Brown SD, Steel KP. Shaker-1 mutations reveal roles for myosin VIIA in both development and function of cochlear hair cells. *Development*. 1998;125:557–566.
17. Hasson T, Walsh J, Cable J, Mooseker MS, Brown SD, Steel KP. Effects of shaker-1 mutations on myosin-VIIa protein and mRNA expression. *Cell Motil Cytoskeleton*. 1997;37:127–138.
18. Liu X, Udovichenko IP, Brown SD, Steel KP, Williams DS. Myosin VIIa participates in opsin transport through the photoreceptor cilium. *J Neurosci*. 1999;19:6267–6274.
19. Rattner A, Sun H, Nathans J. Molecular genetics of human retinal disease. *Annu Rev Genet*. 1999;33:89–131.
20. Hasson T, Heintzelman MB, Santos–Sacchi J, Corey DP, Mooseker MS. Expression in cochlea and retina of myosin VIIa, the gene product defective in Usher syndrome type 1B. *Proc Natl Acad Sci USA*. 1995;92:9815–9819.
21. el-Amraoui A, Sahly I, Picaud S, Sahel J, Abitbol M, Petit C. Human Usher 1B/mouse shaker-1: the retinal phenotype discrepancy explained by the presence/absence of myosin VIIA in the photoreceptor cells. *Hum Mol Genet*. 1996;5:1171–1178.
22. Liu X, Vansant G, Udovichenko IP, Wolfrum U, Williams DS. Myosin VIIa, the product of the Usher 1B syndrome gene, is concentrated in the connecting cilia of photoreceptor cells. *Cell Motil Cytoskeleton*. 1997;37:240–252.
23. Liu X, Ondek B, Williams DS. Mutant myosin VIIa causes defective melanosome distribution in the RPE of shaker-1 mice. *Nat Genet*. 1998;19:117–118.
24. Titus MA. A class VII unconventional myosin is required for phagocytosis. *Curr Biol*. 1999;9:1297–1303.
25. Mburu P, Liu XZ, Walsh J, et al. Mutation analysis of the mouse myosin VIIA deafness gene. *Genes Funct*. 1997;1:191–203.
26. Rinchik EM, Carpenter DA, Selby PB. A strategy for fine-structure functional analysis of a 6- to 11-centimorgan region of mouse chromosome 7 by high-efficiency mutagenesis. *Proc Natl Acad Sci USA*. 1990;87:896–900.
27. Fulton AB, Hansen RM, Findl O. The development of the rod photoresponse from dark-adapted rats. *Invest Ophthalmol Vis Sci*. 1995;36:1038–1045.
28. Brown KT, Wiesel TN. Localization of origins of electroretinogram components by intraretinal recording in the intact cat eye. *J Physiol*. 1961;158:257–280.
29. Penn RD, Hagins WA. Signal transmission along retinal rods and the origin of the electroretinographic a-wave. *Nature*. 1969;223:201–204.
30. Stockton RA, Slaughter MM. B-wave of the electroretinogram: a reflection of ON bipolar cell activity. *J Gen Physiol*. 1989;93:101–122.
31. Gurevich L, Slaughter MM. Comparison of the waveforms of the ON bipolar neuron and the b-wave of the electroretinogram. *Vision Res*. 1993;33:2431–2435.
32. Green DG, Kapousta–Bruneau NV. A dissection of the electroretinogram from the isolated rat retina with microelectrodes and drugs. *Vis Neurosci*. 1999;16:727–41.
33. Lamb TD. Gain and kinetics of activation in the G-protein cascade of phototransduction. *Proc Natl Acad Sci USA*. 1996;93:566–570.
34. Libby RT, Brown SD, Steel KP. Characterisation of retinas of shaker1 mice, a mouse model for Usher syndrome type 1b [ARVO Abstract]. *Invest Ophthalmol Vis Sci*. 1999;38(4):**S**476. Abstract nr 2509.
35. Dowling JE. Chemistry of visual adaptation in the rat. *Nature*. 1960;188:114–118.
36. Dowling JE. Night blindness, dark adaptation and the electroretinogram. *Am J Ophthalmol*. 1960;50:875–889.
37. Williams MA, Pinto LH, Gherson J. The retinal pigment epithelium of wild type (C57BL/6J$^{+/+}$) and pearl mutant (C57BL/6J *pe/pe*) mice. *Invest Ophthalmol Vis Sci*. 1985;26:657–669.
38. Balkema GW Jr, Pinto LH, Drager UC, Vanable JW Jr. Characterization of abnormalities in the visual system of the mutant mouse pearl. *J Neurosci*. 1981;1:1320–1329.
39. Odorizzi G, Cowles CR, Emr SD. The AP-3 complex: a coat of many colours. *Trends Cell Biol.* 1998;8:282–288.
40. Wu X, Jung G, Hammer JA III. Functions of unconventional myosins. *Curr Opin Cell Biol*. 2000; 12:42–51.
41. Emmerling MR, Sobkowicz HM. Acetylcholinesterase-positive innervation in cochleas from two strains of shaker-1 mice. *Hear Res*. 1990;47:25–37.
42. Naash MI, Ripps H, Li S, Goto Y, Peachey NS. Polygenic disease and retinitis pigmentosa: albinism exacerbates photoreceptor degeneration induced by the expression of a mutant opsin in transgenic mice. *J Neurosci*. 1996;16:7853–7858.
43. Danciger M, Matthes MT, Yasamura D, et al. A QTL on distal chromosome 3 that influences the severity of light-induced damage to mouse photoreceptors. *Mamm Genome*. 2000; 11:422–427.
44. Nishina PM, Ikeda A, Naggert JK. Identification of QTLs for protection from photoreceptor cell degeneration in tubby mice [ARVO Abstract]. *Invest Ophthalmol Vis Sci*. 2000;41(4):**S**202. Abstract nr 1057.
45. Kedzierski W, Lloyd M, Birch DG, Bok D, Travis GH. Generation and analysis of transgenic mice expressing P216L-substituted rds/peripherin in rod photoreceptors. *Invest Ophthalmol Vis Sci*. 1997;38:498–509.

46. Chen J, Simon MI, Matthes MT, Yasumura D, LaVail MM. Increased susceptibility to light damage in an arrestin knockout mouse model of Oguchi disease (stationary night blindness). *Invest Ophthalmol Vis Sci*. 1999;40:2978–2982.
47. Chen CK, Burns ME, Spencer M, et al. Abnormal photoresponses and light-induced apoptosis in rods lacking rhodopsin kinase. *Proc Natl Acad Sci USA.* 1999;96:3718–3722.
48. Naash ML, Peachey NS, Li ZY, et al. Light-induced acceleration of photoreceptor degeneration in transgenic mice expressing mutant rhodopsin. *Invest Ophthalmol Vis Sci*. 1996;37:775–782.
49. Mittag TW, Bayer AU, La VM. Light-induced retinal damage in mice carrying a mutated SOD I gene. *Exp Eye Res*. 1999;69:677–683.
50. Sanyal S, Hawkins RK. Development and degeneration of retina in rds mutant mice: effects of light on the rate of degeneration in albino and pigmented homozygous and heterozygous mutant and normal mice. *Vision Res*. 1986;26:1177–1185.
51. LaVail MM, Gorrin GM, Yasumura D, Matthes MT. Increased susceptibility to constant light in nr and pcd mice with inherited retinal degenerations. *Invest Ophthalmol Vis Sci*. 1999;40:1020–1024.
52. Seeliger MW, Apfelstedt-Sylla E, Jaissle GB. ERG implicit time separates Usher syndrome I and II [ARVO Abstract]. *Invest Ophthalmol Vis Sci*. 2000;41(4):**S**332. Abstract nr 4730.